International Research Journal of Engineering and Technology (IRJET) e-ISSN: 2395-0056
Volume: 05 Issue: 12 | Dec 2018 www.irjet.net p-ISSN: 2395-0072

CFD ANALYSIS ON CAR BODY

Daruri Harish[1], K. Veeranjaneyulu[2]

[1]Daruri Harish, Department of Mechanical Engineering, Anurag Engineering College, Kodad, Telangana, India
[2]K. Veeranjaneyulu Associate Professor, Dept. of Mechanical Engineering, Anurag Engineering College, Kodad, Telangana, India

---

Abstract - *With the accentuation lying on expanding eco-friendliness of vehicles so as to battle rising fuel costs and ecological difficulties the makers are thinking past the regular vehicle frameworks by concentrating on its streamlined features. Streamlined drag surpasses 50 percent of the aggregate protection from movement at paces above 70km/hr, or more 100 km/hr it is the most critical factor. The survey is done to distinguish the different weaknesses of the car planners when it is with respect to stream division of air at the back of the vehicle which causes the greater part of the misfortunes. This paper centers around the work officially done in the field of optimal design beginning with Ahmed Body. It is a feign body with flexible back inclination edge and the premise whereupon the aerodynamicists test their models. This conveys to the recreation.. CFD device is discovered exceptionally helpful in car industry extending from framework level (outside streamlined features, ventilation, interior ignition motors) to part level (circle brake cooling).CFD reenactments are completed by partitioning the physical area into little limited volume components and numerically unraveled the overseeing conditions that depict the conduct of the stream.*

The primary worries of car optimal design are decreasing drag, lessening wind commotion, limiting clamor discharge and forestalling undesired lift powers at high speeds. The most critical part in the investigation of autos is to comprehend the weight appropriation over the state of the vehicle. The weight at the back does not recoup to the stagnation weight level. Because of the stream partition, the weights at the back of the vehicle are lower than at the front, which makes drag. For a few classes of hustling vehicles, it might likewise be essential to deliver attractive downwards streamlined powers to enhance footing and in this way cornering capacities. Wind-burrow testing was connected to car, to decide streamlined powers however more to decide approaches to lessen the power required to move the vehicle on roadways at a given speed.

So in this paper we will break down the diverse kinds of vehicle models and their streamlined structures. The principle concern is about the weight and the speed of the distinctive kinds of vehicle bodies. by changing the streamlined shape we will discover the speeds and the weights following up on the bodies.Thus discovering whether the body can withstand the weight and speed at a specific given arrangement of conditions. Consequently the productivity of the vehicle is controlled by the streamlined structure and state of the vehicle body.

1. INTRODUCTION

Aerodynamics speaks to an uncommon logical documented that huge affects present day car building. Optimal design manages the impact of outer factors on the watched question, and also the state of the protest so as to accomplish the ideal execution. The optimal design powers and coefficients vigorously impact the conduct of vehicles out and about. The principle three optimal design powers are Drag Force, Lift Force and Lateral Force. Every one of these forces has angular rotation around its axis, that are Roll, Pitch and Yaw. This vehicle demonstrate was made on the real model and its specialized documentation. In the wake of displaying, testing office was presented in a streamlined form of the wind tunel, in which the methods for reproductions played out a point by point examination of the effect of the outer factors regarding the matter. From that point onward, the outcomes are broke down and examinations and confirmation of numerical calculations for that vehicle are performed.

1.1 Car 3D model and renderings

The car model is madewith the software Autodesk 3ds Max. Polyg-onal modeling method was used for creating the car geometry. The final model with all details consists of 507 984 polygons and 568 254 vertexes. The polygonal model is presented in Figure 1.

1.2 Computational Fluid Dynamics (CFD)

To analyze the aerodynamic features of vehicles there are two possibilities and especially the turbulences: the wind tunnel and computational fluid dynamics (CFD). The better solution for efficiency and the financial aspect is CFD. Even the visualization and the accuracy are other aspects which show the advantages of CFD. New turbulence models and the increasing computing power make CFD much more important.

For air-flow around the car Finite volume method (FVM) was used. For 2D analysis of the airflow around the side contour of a car, the software GAMBIT was used as preprocessor for modeling and discretization of the problem, and the software FLUENT was used as solver and postprocessor. ANSYS CFX was used for 3D analysis of the airflow around the car geometry.

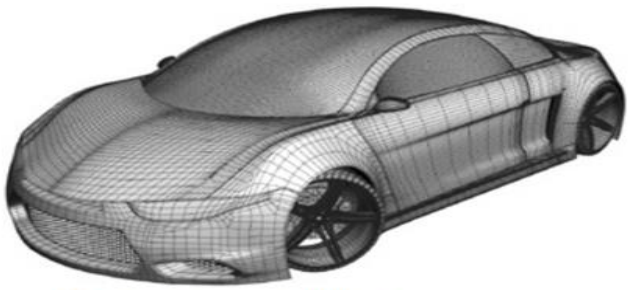

Figure 1: Polygonal car model

2. Theory

The governing conditions for computational liquid dynamics always depend on conservation of mass, momentum and energy. Both FLUENT and ANSYS CFX utilize a FVM to evaluate the governing conditions. The FVM includes discretization and integartion of the governing equations over the finite volume.

The stream is said to be fierce when all the vehicle amounts (mass, force and vitality) display intermittent, sporadic fluctua-tions in existence. Such conditions upgrade blending of these vehicle factors. There is no single violent model that can resolve the material science at all stream conditions. Familiar and ANSYS CFX gives a wide assortment of models to suit the requests of individual classes of issues. The decision of the violent model relies upon the required dimension of precision, the accessible computational assets and the required turnaround time.

For the issue dissected in this paper, standard k - ε tur-bulent demonstrate is chosen for both 2D and 3D investigation. The k - ε demonstrate is a standout amongst the most widely recognized violent models. It is a semi - observational, two-condition demonstrate, which implies, it incorporates two additional vehicle conditions to speak to the tempestuous properties of the stream. The primary transport variable is the fierce motor vitality k. The second transport variable is the tempestuous scattering ε. The variable decides the size of the disturbance, while the main variable k decides the vitality in the choppiness.

The model transport condition for k is gotten from the correct condition, while the model transport condition for k is acquired utilizing physical thinking and looks to some extent like its scientifically counterpart.

2.1 Governing Equations

The continuity and momentum equations (Navier - Stokes equations) with a turbulence model were used to solve the airflow.

$$\frac{\partial u}{\partial x}+\frac{\partial v}{\partial y}+\frac{\partial w}{\partial z}=0, \quad (1)$$

$$u\frac{\partial u}{\partial x}+v\frac{\partial u}{\partial y}+w\frac{\partial u}{\partial z}=-\frac{1}{\rho}\frac{\partial p}{\partial x}+\frac{1}{\rho}\left(\frac{\partial \tau_{xy}}{\partial y}+\frac{\partial \tau_{xz}}{\partial z}\right)+B_x, \quad (2)$$

$$u\frac{\partial v}{\partial x}+v\frac{\partial v}{\partial y}+w\frac{\partial v}{\partial z}=-\frac{1}{\rho}\frac{\partial p}{\partial y}+\frac{1}{\rho}\left(\frac{\partial \tau_{xy}}{\partial x}+\frac{\partial \tau_{yz}}{\partial z}\right)+B_y, \quad (3)$$

$$u\frac{\partial w}{\partial x}+v\frac{\partial w}{\partial y}+w\frac{\partial w}{\partial z}=-\frac{1}{\rho}\frac{\partial p}{\partial z}+\frac{1}{\rho}\left(\frac{\partial \tau_{xz}}{\partial x}+\frac{\partial \tau_{yz}}{\partial y}\right)+B_z. \quad (4)$$

Where u is x - component of velocity vector, v is y - component of velocity vector and w is z - component of velocity vector. ρ is density of air, p is static pressure, τ is shear stress and B_x, B_y, B_z are body forces.

2.1.2 Transport Equations for standard k - ε turbulent model - for turbulent kinetic energy k:

$$\frac{\partial}{\partial t}(\rho k)+\frac{\partial}{\partial x_i}(\rho k u_i)=\frac{\partial}{\partial x_j}\left[\left(\mu+\frac{\mu_t}{\sigma_k}\right)\frac{\partial k}{\partial x_j}\right]+G_k+G_b-\rho\varepsilon-Y_M+S_k \quad (5)$$

-for dissipation ε:

$$\frac{\partial}{\partial t}(\rho \varepsilon)+\frac{\partial}{\partial x_i}(\rho \varepsilon u_i)=\frac{\partial}{\partial x_j}\left[\left(\mu+\frac{\mu_t}{\sigma_\varepsilon}\right)\frac{\partial \varepsilon}{\partial x_j}\right]+C_{1\varepsilon}\frac{\varepsilon}{k}(G_k+C_{3\varepsilon}G_b)-C_{2\varepsilon}\rho\frac{\varepsilon^2}{k}+S_\varepsilon \quad (6)$$

In these equations, Gk represents the generation of turbulence kinetic energy due to the mean velocity gradients. Gb is the generation of turbulence kinetic energy due to buoyancy. YM represents the contribution of the fluctuating dilatation in compressible turbulence to the overall dissipation rate. C1e, C2e and C3e are constants. σk and σe are the turbulent Prandtl numbers for k and ε, respectively. Sk and Se are user-defined source terms.

2.1.3 Turbulent

$$\mu_t=\rho C_\mu\frac{k^2}{\varepsilon} \quad (7)$$

where Cμ is constant

2.1.4 Production of turbulent kinetic energy

From the exact equation for the transport of k, this term may
be defined as:

$$G_k=-\rho\,\overline{u_i'u_j'}\frac{\partial u_j}{\partial x_i} \quad (8)$$

To evaluate G_k in a manner consistent with the Boussinesq hypothesis,:

$G_k = \mu_t S^2$, (9)

where *S* is the modulus of the mean rate - of - strain tensor, defined as:

$$S \equiv \sqrt{2S_{ij}S_{ij}}\,, \tag{10}$$

Where

$$S_{ij} = \frac{1}{2}\left(\frac{\partial u_i}{\partial u_j} + \frac{\partial u_j}{\partial u_i}\right) \text{ [5].} \tag{11}$$

2.1.5 The generation of turbulence due to buoyancy

$$G_b = \beta g_i \frac{\mu_t}{Pr_t}\frac{\partial T}{\partial x_i}\,, \tag{12}$$

where Pr_t is the turbulent Prandtl number for energy and gi is the component of the gravitational vector in the *i* - th direction. For the standard and realizable models, the default value of Pr_t is 0.85.

The coefficient of thermal expansion β is defined as:

$$\beta = -\frac{1}{\rho}\left(\frac{\partial p}{\partial T}\right)_p \text{ [5].} \tag{13}$$

2.1.6 The dilatation dissipation

The dilatation dissipation term YM, is included in the k equation. This term is modeled according to:

$$Y_M = 2\rho \varepsilon M_t^2 \tag{14}$$

where M^2 is the turbulent mach number, defined as:

$$M_t = \sqrt{\frac{k}{a^2}} \tag{15}$$

where *a* is the speed of sound:

$$a \equiv \sqrt{\gamma RT} \text{ [5].} \tag{16}$$

2.1.6 Model constants

The model constants C1e, C2e, Cμ, σk and σe have the following default values:

C1e = 1.44, C2e = 1.92, Cμ = 0.09, σk = 1.0, σe = 1.3.

These default values have been determined from experiments with air and water for fundamental turbulent shear flows including homogeneous shear flows and decaying isotropic grid turbulence. They have been found to work fairly well for a wide range of wall- bounded and free shear flows.

3. Two-dimensional CFD analysis of side contour of the car

2D analysis are exceptionally useful and for the most part gone before by a 3D investigation, since they can give some essential rules that could be updated on the item all together that the subsequent 3D analysis give better and progressively worthy outcomes. This methodology can essentially abbreviate the season of examining an issue, in light of the fact that the 2D examination in connection to 3D is obviously a lot less difficult and the time for getting an answer is a lot shorter. In this way, the 2D investigation is a decent marker of the genuine state, anyway it is important to take note of that the outcomes could fundamentally change when the equivalent issue is considered in 3D.

3.1 Discretization of the 2D domain

After meshing problem in GAMBIT, the mesh consists of quads and triangulars. As Figures 3 and 4 show, the mesh is discretized as organized near the vehicle shape and on the best and the base of the area as well. Measurements of investigation space are introduced in Figure 2, where L = 4500 mm.

As referenced before, two instances of vehicle geometry was analyzed. The main case is the underlying plan, so the geometry of the current model and the second case are overhauled geometry regarding expanding the edge between the hood and the front windshield to improve wind stream around the vehicle. Additionally, in the updated vehicle geometry, raise wing is included the reason to see changes and investigate wind stream with the back wing. Figure 3 demonstrates the limited volume work of the principal instance of vehicle geometry and Figure 4 demonstrates the second instance of vehicle geometry with the referenced changes.

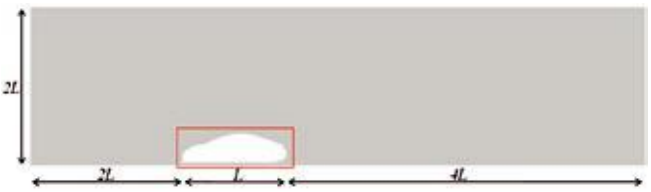

Figure 2: Dimensions and discretization of 2D domain

Figure 3: Finite volume mesh of the first case of car geometry (initial car geometry).

3.2 Boundary conditions

Speed of the air at the gulf limit condition is set in FLUENT with an estimation of 27,7 m/s (≈100 km/h) and with a tem-perature of 300 K (≈26,85oC). The outlet limit condition is set to weight outlet with the check weight of 0 Pa. The vehicle shape, the best and the base of the virtual breeze burrow are set as dividers. The thickness of air is set as 1.225 kg/m3 and the consistency of air is 1.7894 x 10-5 kg/(ms).

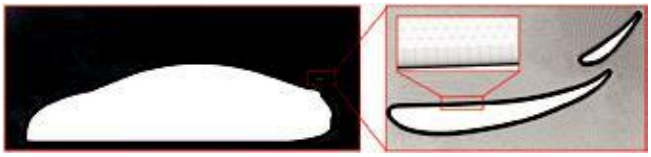

Figure 4: Finite volume mesh of the second case of car geometry (redesigned geometry)

3.3 Results

Figure 5 demonstrates the speed forms of the underlying vehicle geometry, and Figure 6 demonstrates the speed shapes of the updated vehicle geometry. Figures demonstrate that the air speed is diminishing as it is moving toward the front of the vehicle. At that point air speed increments from the vehicle front. In the second case, the speed extent increments with a higher inclination, which implies that the air opposition is littler.

Figures 7 and 8 indicates static weight shapes. It is clear from the Figures that there is a higher weight fixation on the vehicle front in the two cases, and at the back wing in the second case. Especially, the air backs off when it approaches the front of the vehicle and results in that more air particles are gathered into a littler space. When the air stagnates before the vehicle, it looks for a lower weight territory, for example, the sides, top and the base of the vehicle. As the wind streams over the vehicle hood, weight is diminishing, however when achieves the front windshield, it increments quickly. At the point when the higher-weight air before the windshield goes over the windshield, it quickens, causing the decline of the weight. This lower weight truly creates a lift - constrain on the vehicle rooftop as the air ignores it. Additionally, Figure 8 demonstrates that there is a bigger measure of weight on the best surface of the back wing. That weight is creating a greater down - constrain bringing about better strength of the vehicle and expanding footing. The wing is an exceptionally proficient streamlined include - in, on the grounds that it makes heaps of down - compel and along these lines with little impact to expanding drag.

Figures 9 and 10 indicate choppiness power shapes + vectors for the two instances of vehicle geometry. It is clear from the displayed Figures that the back wing has enormous hugeness to the turbulences. It tends to be seen that if there should arise an occurrence of the overhauled vehicle geometry there is less turbulences behind the vehicle and the fierce zone is more clean.

Figure 5: Velocity contours over the initial car geometry (first case)

Figure 6: Velocity contours over the redesigned car geometry (second case)

Figure 7: Static pressure contours over the initial car geometry (case one)

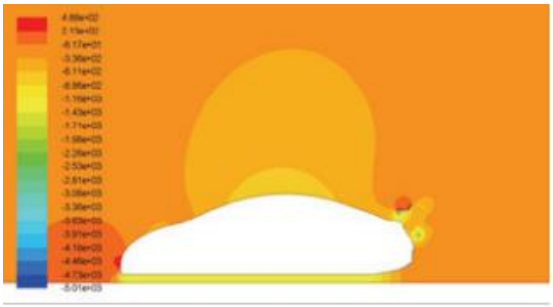

Figure 8: Static pressure contours over the redesigned car geometry (case two)

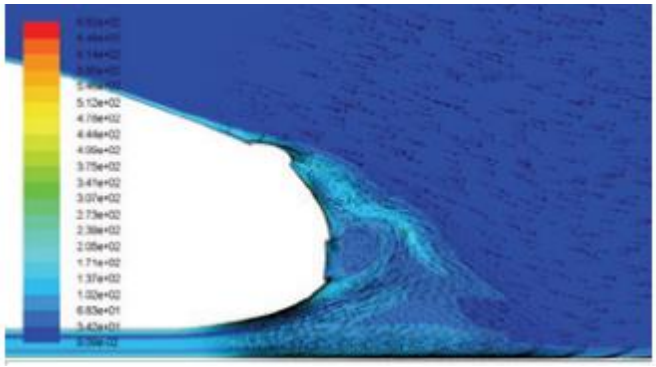

Figure 9: Turbulence intensity contours + vectors over the initial car geometry (first case)

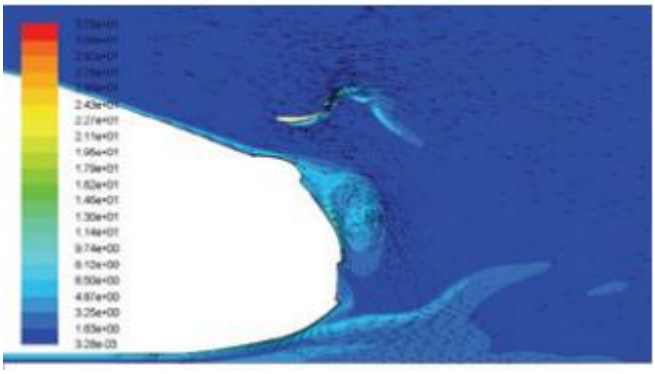

Figure 10: Turbulence intensity contours + vectors over the redesigned car geometry (second case)

Figure 11: Design of the rear wing

Figure 11.1: Design of the rear wing

4. Redesigned car model

Prompting the changes of a current model regarding the upgraded side form of the vehicle and driving with the acquired 2D aftereffects of the wind stream around the vehicle, the current 3D vehicle demonstrate has been updated. The new model has a marginally bigger number of polygons because of the additional back wing. In the wake of applying materials and surfaces to each piece of vehicle and scene, each photo takes around 2,5 hour for rendering. The psychological Ray rendering apparatus was utilized for rendering as a default rendering instrument of Autodesk 3ds Max.

Figure 11 demonstrates the plan of the back wing, and Figure 12 demonstrates a portion of the renderings of the new, redesigned car model

5. Three dimensional CFD analysis of car

Likewise for this situation, the two geometries of the vehicle were broke down. A few subtleties, for example, vehicle wheels, breaks, exhaust, and so on are arranged from the 3D investigation in the motivation behind rearranging the model and the examination as well. Notwithstanding, regardless of the reality of that the model comprises of very number of components.

5.1 Discretization of the 3D domain

Because of the full symmetry of the issue, just a single portion of the space is coincided and subsequent to cross section the area in ANSYS, the work comprises of 1874264 hubs and 6148164 components in the event of the underlying vehicle geometry, and of 2854713 hubs and 9560271 components if there should arise an occurrence of the updated vehicle geometry. Figure 13 indicates measurements of the examination space, where L = 4500 mm. The work is discretized as organized near the vehicle form and on the base of space as well. Figure 14 demonstrates the surface work of the full fit space, and Figure 15 demonstrates some surface work subtleties of the organized work around the vehicle geometry.

As on account of the 2D examination, to get the most exact outcomes and inside the most indistinguishable conditions, the work is dis-cretized in the two instances of the geometry with a similar thickness. The main contrast is that if there should arise an occurrence of the updated vehicle geometry, the work has a higher number of components. That is on the grounds that the back wing is included the overhauled vehicle geometry, and the work is created around it with greater thickness, Figure 16 and 17. Figure 16 and 17 demonstrate the volume work and a few subtleties of the organized volume work around the back wing and the side mirror.

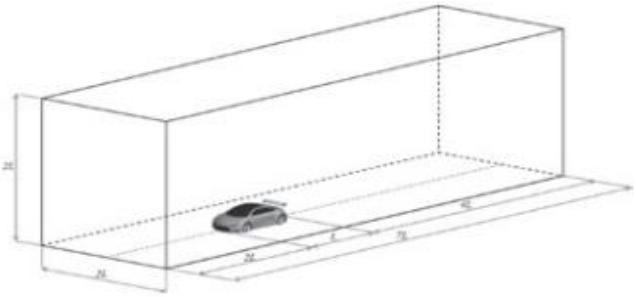

Figure 13: Dimensions of the 3D domain

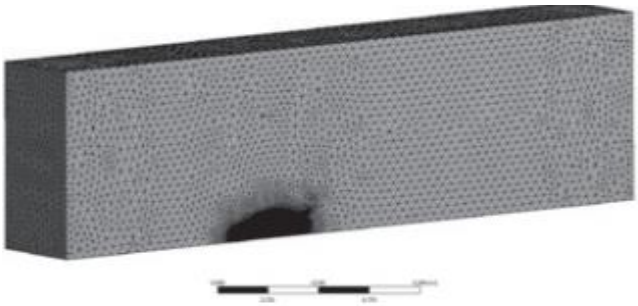

Figure 14: The meshed domain

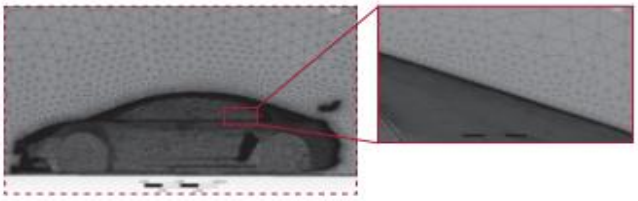

Figure 15: Surface mesh of the domain

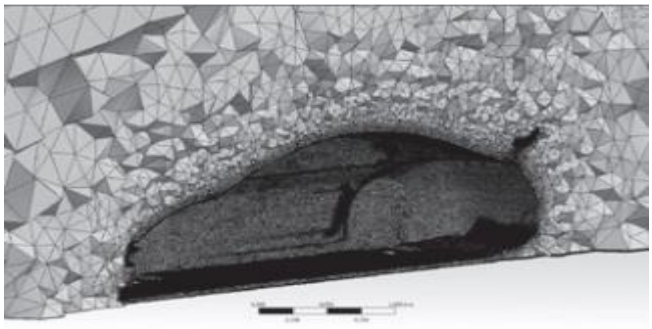

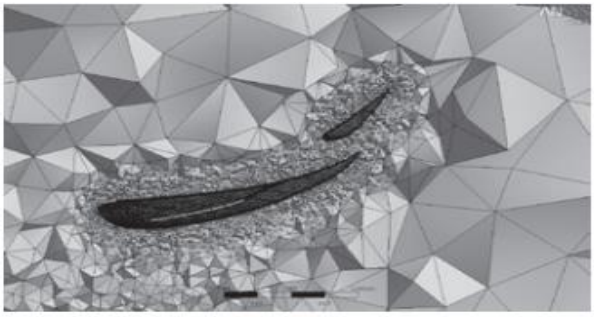

Figure 16: Details of the finite volume mesh around the car geometry

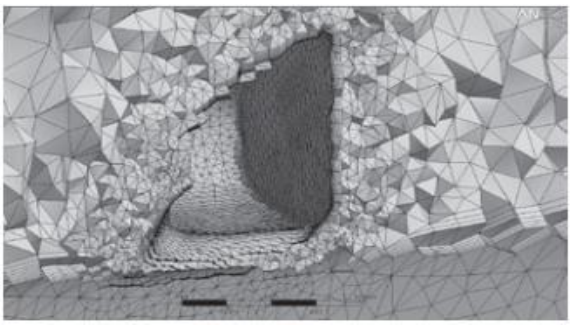

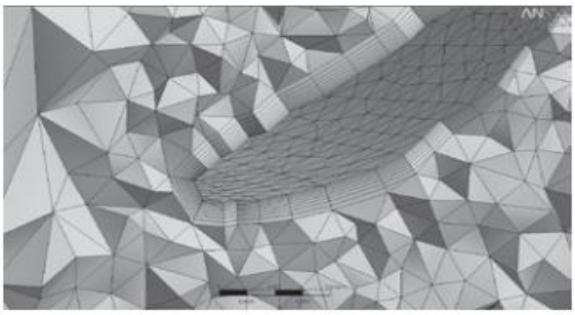

Figure 17: Details of the structured mesh on the side mirror and the rear wing

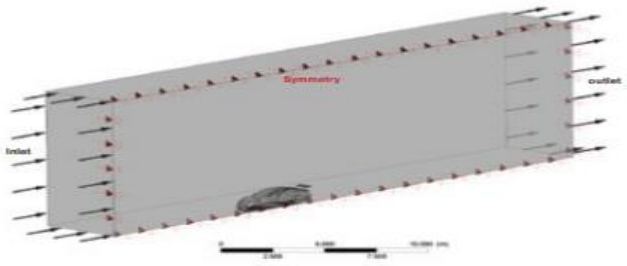

Figure 18: Boundary conditions of the 3D domain

5.2 Boundary conditions

The material is set as "Air Ideal Gas" and the speed of the air at the channel limit condition is set in ANSYS CFX with an estimation of 27,7 m/s (≈100 km/h) and with a temperature of 300 K (≈26,85oC). The k - ε turbulent model is chosen. The entire vehicle body and the base of the virtual wind tunnel are set as smooth divider with the alternative of "No Slip Wall". The best and the side of the passage are set as "Wall" with the choice of "Free Slip Wall". The outlet limit condition is set to "Outlet" with the relative static weight of 0 Pa. Furthermore, the "Symmetry" boundary condition is set to the symmetry plane. Figure 17 demonstrates the limit states of the 3D space (Figure 18).

Figure 12: Renderings of the redesigned car model

5.3 Results

Tragically, because of the absence of PC gear, the geometry of the vehicle is disentangled, and along these lines the CFD examination, so in addition to other things, the wheels are shot out from the investigation. In a further work, the point is to make a CFD reproduction of a vehicle in movement, so with turning haggles ground. Likewise in the performed investigation, the section of the air into the front and the side air admissions are not mulled over, which very changes a practical image of the outcomes, so in a further work, we will probably think about that as well. Figure 19 demonstrates the weight conveyance on 3D model of the vehicle and the ground from front and back of the vehicle. Not surprisingly, from weight shapes clearly there is a bigger weight sum before the vehicle, particularly at the front and the side air admissions. In the event of the updated vehicle geometry, the most extreme weight sum is on the best surface of the back wing, and the consequence of that is creating a down - compel. How wings produce down – constrain, will be talked about henceforth. Figures from 20 to 22 indicates speed streamlines over both vehicle geometries, from various blessed messengers and for some individual parts of the vehicle. Figure 22 indicates speed streamlines beneath the vehicle. As appeared in the 2D investigation, by and by, it is affirmed that by including a back wing a vehicle, there is less turbulences behind the vehicle. It is likewise ob-vious that the speed streamlines by removing from the underlying vehicle geometry are growing, while in the contrary circumstance, if there should be an occurrence of a vehicle with back wing, speed streamlines are narrowing. This implies the tempestuous zone behind the upgraded vehicle is littler. More choppiness behind the underlying vehicle geometry is likewise evident from Figure 21, which introduces the speed streamlines on the symmetry plane, so the eddy's are easier to see. The purpose behind the growing of speed streamlines on account of geometry without back wing is that the air in the wake of disregarding the back windshield goes straightforwardly to the ground. That air has a higher speed and comes into impact behind the vehicle with the air from beneath the vehicle which has a lower speed. So the growing of speed streamlines are caused by removing from the vehicle. By utilizing the back wing, the inverse happens, in light of the fact that the wind current is coordinating upwards by the back wing and therefore permits slower air from beneath the vehicle to free stream by removing from the vehicle, so there is no extending of the wind current, Figure 22. Figure 23 demonstrates the speed and the weight conveyance over the back wing. The back wings are about unimportant in customary passenger autos, yet with regards to sports vehicles, particularly those for race, these are the most essential streamlined include - ins. For instance, for a F1 vehicle, the back wing makes around third of the vehicle down - constrain.

But running at high speeds the drag from the back wing is colossal. It would be the best to accomplish the accompanying: progressively down - drive at lower speeds in the motivation behind expanding footing and consequently better increasing speed, and less down – constrain at higher rates when the vehicle is on a straight line and doesn't require down – force.

A wing creates down - constrain because of its profile quickening wind current on its lower surface in connection to the stream over the best sur-confront. In the event that the stream is quickened, the weight is diminishing, bringing about a weight differential between the upper and lower surface of the wing and hence producing a down - constrain. As the wind streams over the surface of a wing, it tends to back off and separate from the wing, especially underneath the wing which keeps running at a lower weight than the best surface, Figure 23. This detachment at first diminishes proficiency and the wind current absolutely separates and the wing slows down. At the point when a wing slows down, it loses the greater part of its down - compel (that is required at higher rates). Be that as

it may, at lower speeds, the point is to avoid detachment. So it is expected to accelerate the stream close to the wingsurface. To accomplish both, double component wings are utilized, Figure 23. These take into consideration a portion of the high weight spill out of the best surface of the lower wing to seep to the lower surface of the upper wing. This builds the wind current speed under the wing, expanding down – power and diminishing the limit stream partition.

Something else, in light of the fact that there is an expanded stacking that accompanies higher speeds on the straight and due to flexi upper wing it will divert (or simply part of it), and hence the upper wing will draw nearer to the lower wing bringing about the hole between them becom-ing littler. This prompts the partition and wing slows down, so sheds down – compel and with that drag. So as to demonstrate this, the 2D reproduction of the wind current around the side form of the vehicle was made for the speed of 250 km/h, in light of the fact that the supposition is that at this speed the upper wing will avoid and draw nearer to the lower wing. Figure 24 demonstrates that this prompts the partition and the wing slows down. Be that as it may, the inquiry is: "How such structure of the back wing influences the streamlined drag – drive"? Definitely, this sort of back wing expands drag – compel at higher velocities. Along these lines, by various investigation, (CFD and examination in wind burrow) it is important to discover the trading off arrangement which will diminish enough down – drive at the higher velocities, however of the sometime doesn't impact the expansion of the drag – constrain extraordinarily.

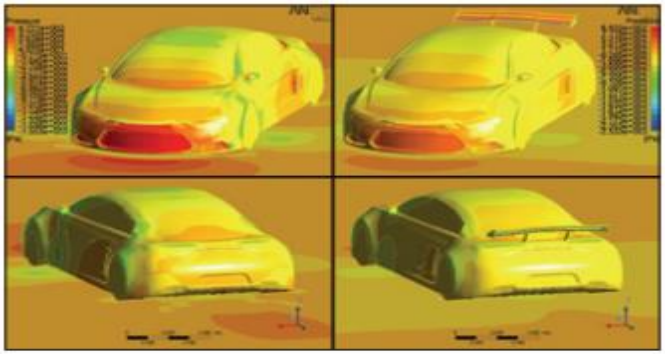

Figure 19: Pressure distribution on the car body and the ground

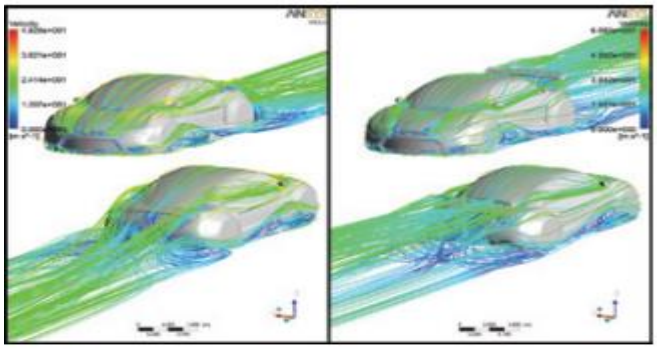

Figure 20: Velocity streamlines over the car body

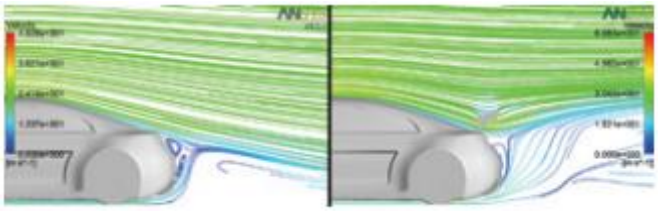

Figure 21: Velocity streamlines on the symmetry plane of the car

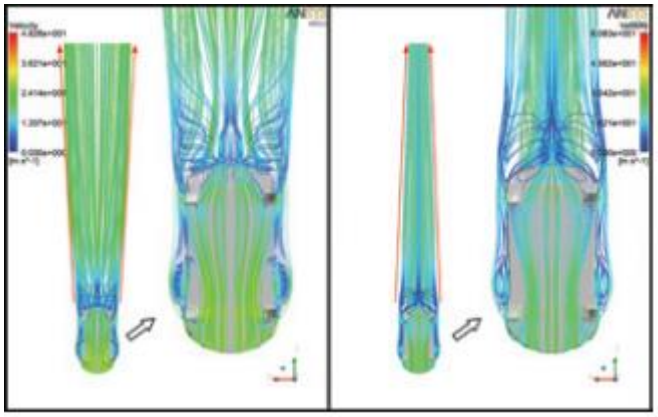

Figure 22: Velocity streamlines from below the car

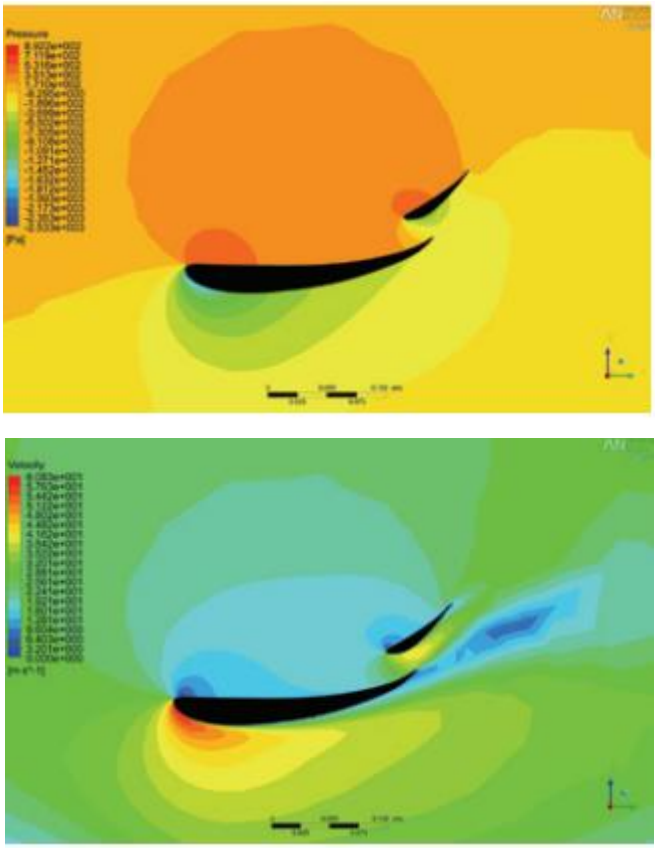

Figure 23: Pressure and velocity contours over the rear wing, deflecting of upper wing

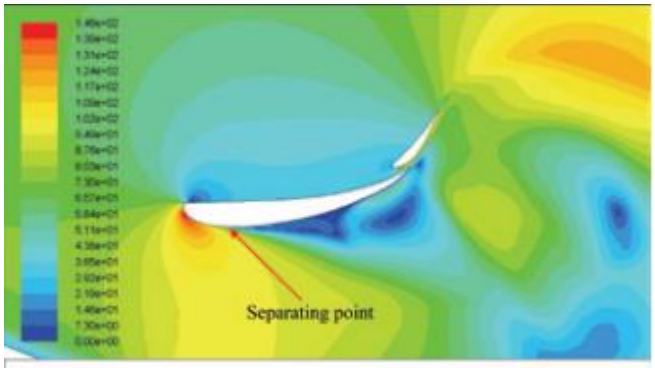

Figure 24: Velocity contours over the rear wing at speed of 250 km/h

6. Conclusions

Based on the vehicle model, 2D and 3D reenactments were performed for both vehicle geometries to picture the wind current and weight appropriation. The referenced CFD investigations are accomplished to see basic places in geometry which are bringing about awful streamlined features. Prompting the got 2D recreation and driving with alterations of a current 2D show as far as the updated side form of the vehicle, the current 3D vehicle display is upgraded. Update is as far as expanding edge between the hood and the front windshield of the vehicle, and including the back wing. Moreover, the 3D examination of wind current around the overhauled vehicle geometry was accomplished. With the got 2D and 3D results, it is closed that the referenced changes in the geometry of the overhauled vehicle are bringing about better wind current around the vehicle, and creating more down – constrain utilizing the back wing. Greater measure of down – force is bringing about better dependability of the vehicle and the expanding footing. A double component wing is utilized on account of the likelihood to accomplish increasingly down – drive at lower speeds in the reason for expanding footing and in this way better quickening and less down – compel at higher rates when vehicle is on a straight line and doesn't require a down – drive. Wings are extremely proficient streamlined add – ins, since they make a great deal of down – drive and along these lines with little impact on the expanding drag. It is additionally settled that in instance of the upgraded vehicle geometry there is less turbulences behind the vehicle and the tempestuous zone is cleaner. Because of the perception that double component raise wings are expanding drag - compel at higher rates, it is important to discover the bargaining arrangement which will lessen enough the down – constrain at the higher paces, however at the sometime doesn't impact the expanding of drag – force significantly.

References

[1] http://www.autozine.org/technical_school/aero/tech_aero.htm (17.06.2010)

[2] Milad Mafi, "Investigation of Turbulence Created by Formula One™ Cars with the Aid of Numerical Fluid Dynamics and Optimization of Overtaking Potential", Competence Centre, Transtec AG, Tübingen, Germany

[3] Virag, Zdravko, Lectures from the course "Numerical methods"

[4] Luke Jongebloed, "Numerical Study using FLUENT of the Separation and Reattachment Points for Backwards - Facing Step Flow", Me-chanical Engineering Rensselaer Polytechnic Institute, Hartford, Connecticut, December, 2008

[5] ANSYS Fluent, Release 12.1: Help Topics

[6] http://www.up22.com/Aerodynamics.htm (25.07.2010)

[7] http://scarbsf1.wordpress.com/2010/03/04/blown-rear-wings-separating-and-stalling/ (07.09.2010)

[8] http://www.racecar-engineering.com/articles/f1/449813/f-ducts-how-do-they- work.html (08.09.2010)

[9] Popat, B.C., 1991. Study of Flow and Noise Generation from Car A-pillars, Ph.D. Thesis, Department of Aeronautics, Imperial College of Science, Technology and Medicine, The University of London, UK.